AXONAL DEGENERATION

RIPK1 mediates axonal degeneration by promoting inflammation and necroptosis in ALS

Yasushi Ito,[1] Dimitry Ofengeim,[1] Ayaz Najafov,[1] Sudeshna Das,[2] Shahram Saberi,[3,4] Ying Li,[1,5] Junichi Hitomi,[1] Hong Zhu,[1] Hongbo Chen,[1] Lior Mayo,[6] Jiefei Geng,[1] Palak Amin,[1] Judy Park DeWitt,[1] Adnan Kasim Mookhtiar,[1] Marcus Florez,[1] Amanda Tomie Ouchida,[1] Jian-bing Fan,[7] Manolis Pasparakis,[8] Michelle A. Kelliher,[9] John Ravits,[3,4] Junying Yuan[1,5]*

Mutations in the *optineurin* (*OPTN*) gene have been implicated in both familial and sporadic amyotrophic lateral sclerosis (ALS). However, the role of this protein in the central nervous system (CNS) and how it may contribute to ALS pathology are unclear. Here, we found that optineurin actively suppressed receptor-interacting kinase 1 (RIPK1)–dependent signaling by regulating its turnover. Loss of OPTN led to progressive dysmyelination and axonal degeneration through engagement of necroptotic machinery in the CNS, including RIPK1, RIPK3, and mixed lineage kinase domain–like protein (MLKL). Furthermore, RIPK1- and RIPK3-mediated axonal pathology was commonly observed in *SOD1*^{G93A} transgenic mice and pathological samples from human ALS patients. Thus, RIPK1 and RIPK3 play a critical role in mediating progressive axonal degeneration. Furthermore, inhibiting RIPK1 kinase may provide an axonal protective strategy for the treatment of ALS and other human degenerative diseases characterized by axonal degeneration.

Loss-of-function mutations in the *optineurin* (*OPTN*) gene have been implicated in both familial and sporadic cases of amyotrophic lateral sclerosis (ALS), a devastating degenerative motor neuron disease (*1*–*3*). The *Optn* gene encodes a ubiquitin-binding protein involved in tumor necrosis factor–α (TNFα) signaling but is dispensable for nuclear factor κB (NF-κB) activation (*4*, *5*). It is still unclear how the loss of function of *OPTN* leads to human ALS.

Receptor-interacting kinase 1 (RIPK1) is a critical regulator of cell death and inflammation (*6*). RIPK1 regulates necroptosis, a form of regulated necrotic cell death, by promoting the sequential activation of two downstream targets, RIPK3 and mixed lineage kinase domain–like protein (MLKL) (*7*–*9*). Application of necrostatin-1 (7-Cl-O-Nec-1) (Nec-1s), a highly specific inhibitor of RIPK1 kinase activity, blocks necroptosis and inflammation in vitro and in vivo (*10*, *11*). However, the pathophysiological significance of RIPK1 and necroptosis in the genetic context of human diseases remains to be established.

ALS belongs to axonal "dying back" neurodegenerative diseases, as the onset begins with axonal pathology. Axonal degeneration makes a substantial contribution to neurological disability in these patients (*12*). Axonal degeneration induced by direct nerve injury—known as Wallerian degeneration—is mediated through a mechanism distinct from apoptosis of neuronal cell bodies (*13*, *14*). Axonal degeneration in patients with neurodegenerative diseases such as ALS may also exhibit features similar to those of Wallerian degeneration and is referred to as "Wallerian-like" degeneration. The mechanism of Wallerian or Wallerian-like degeneration is still unclear.

To understand the mechanism by which the loss of OPTN could lead to ALS, we developed *Optn*$^{-/-}$ mice (fig. S1, A and B). We examined the impact of *Optn* loss in the spinal cord of *Optn*$^{-/-}$ mice. The number and morphology of spinal cord motor neurons in *Optn*$^{-/-}$ mice were indistinguishable from wild-type (WT) mice (fig. S1, C and D). However, from the age of 3 weeks to 2 years, we observed a marked reduction in the number of motor axons and abnormal myelination in the ventrolateral spinal cord white matter in the *Optn*$^{-/-}$ mice (Fig. 1, A to D, and fig. S1E). The axonal pathology presented as a decompaction of myelin sheaths with a decreased g-ratio (axon diameter/axon-plus-myelin diameter), an increased number of large-diameter axons, and a decreased axonal number in the ventrolateral white matter (Fig. 1, B to D), which suggested degeneration and swelling of motor neuron axons in *Optn*$^{-/-}$ mice. This finding is similar to the axonal pathology observed in the spinal cords of ALS patients in the early stages of the disease (*15*). The pathology was progressive—a reduction in axonal numbers was observed at 12 weeks or older but not at 3 weeks (fig. S1F). Similar pathology was observed in the ventral roots of motor axons in *Optn*$^{-/-}$ mice (fig. S1, G to J). In addition, denervation of neuromuscular junctions in the tibialis anterior muscle was observed in *Optn*$^{-/-}$ mice (fig. S1, K and L). Thus, OPTN deficiency leads to axonal pathology without affecting motor neuron cell bodies. Consistent with this notion, we observed a significant increase in the number of cells positive for terminal deoxynucleotidyl transferase–mediated deoxyuridine triphosphate nick end labeling (TUNEL^{+} cells) in the ventrolateral white matter of spinal cords of *Optn*$^{-/-}$ mice (Fig. 1E). Thus, Optn deficiency sensitizes cells to cell death in the spinal cord white matter of *Optn*$^{-/-}$ mice.

To determine the cell types involved in mediating Optn deficiency–induced axonal degeneration, we generated lineage-specific deletion of Optn using *Cnp-cre*, *Lyz2-cre*, *Gfap-cre*, and *Mnx1-cre* mice (*16*–*18*) (fig. S2). Loss of Optn from oligodendrocytes and myeloid cells, but not from astrocytes or motor neurons, was sufficient to reproduce axonal myelination pathology (Fig. 1, F to I). Furthermore, we induced Optn loss from the microglial lineage by dosing *Optn*$^{F/F}$;*Cx3cr1*^{Cre} mice (*19*) with tamoxifen for 1 month (fig. S3A) and also found axonal pathology like that in *Optn*$^{-/-}$ mice (fig. S3, B to E).

We found that knockdown of Optn sensitized cells to necroptosis in our genome-wide small interfering RNA screen (*20*, *21*) (Z-score = –2.07) (table S1). We further confirmed that knockdown of *Optn* sensitized L929 cells to necroptosis induced by TNFα or zVAD.fmk (fig. S4, A and B). zVAD-induced necrosis is known to involve autocrine TNFα activity (*22*). Thus, *Optn* deficiency sensitized cells to necroptosis (fig. S4C). The biochemical hallmarks of necroptosis—including the upshifts of Ripk1, Ripk3, and phospho-MLKL (p-MLKL), as well as the levels of complex IIb—were significantly higher in *Optn*$^{-/-}$ mouse embryo fibroblasts (MEFs) than in *Optn*$^{+/+}$ MEFs stimulated by TNFα, zVAD, or cycloheximide (fig. S4D). Note that *Optn*$^{-/-}$ oligodendrocytes were sensitized to die by TNFα-induced necroptosis but were protected by Nec-1s and in *Optn*$^{-/-}$;*Ripk1*$^{D138N/D138N}$ and *Optn*$^{-/-}$;*Ripk3*$^{-/-}$ double mutants (*23*, *24*) (Fig. 2A). Thus, Optn deficiency can promote necroptosis of oligodendrocytes.

The expression levels of Ripk1, Ripk3, and MLKL—the key mediators of necroptosis—were all increased in the spinal cords of *Optn*$^{-/-}$ mice (Fig. 2B). Furthermore, we detected the interaction of Optn and Ripk1 in spinal cords from WT mice (Fig. 2C). Compared with WT mice, RIPK1 lysine 48 (K48) ubiquitination levels were decreased, whereas Ripk1 mRNA was unchanged in the spinal cords of *Optn*$^{-/-}$ mice (Fig. 2, D and E). Furthermore, Ripk1 was degraded more slowly in *Optn*$^{-/-}$ MEFs than that in WT cells

[1]Department of Cell Biology, Harvard Medical School, 240 Longwood Avenue, Boston, MA 02115, USA. [2]MassGeneral Institute for Neurodegenerative Disease, Massachusetts General Hospital, Cambridge, MA 02139, USA. [3]Department of Neurology, Harvard Medical School, Boston, MA 02115, USA. [4]ALS Translational Research Program, Department of Neurosciences, University of California, San Diego, La Jolla, CA 92093, USA. [5]Interdisciplinary Research Center on Biology and Chemistry, Shanghai Institute of Organic Chemistry, Chinese Academy of Sciences, 26 QiuYue Road, PuDong District, Shanghai, 201210, China. [6]Ann Romney Center for Neurologic Diseases, Brigham and Women's Hospital, Harvard Medical School, Boston, MA 02115, USA. [7]Illumina, Inc., San Diego, CA 92122, USA. [8]Institute for Genetics, University of Cologne, 50674 Cologne, Germany. [9]Department of Cancer Biology, University of Massachusetts Medical School, Worcester, MA 01605, USA.
*Corresponding author. Email: jyuan@hms.harvard.edu

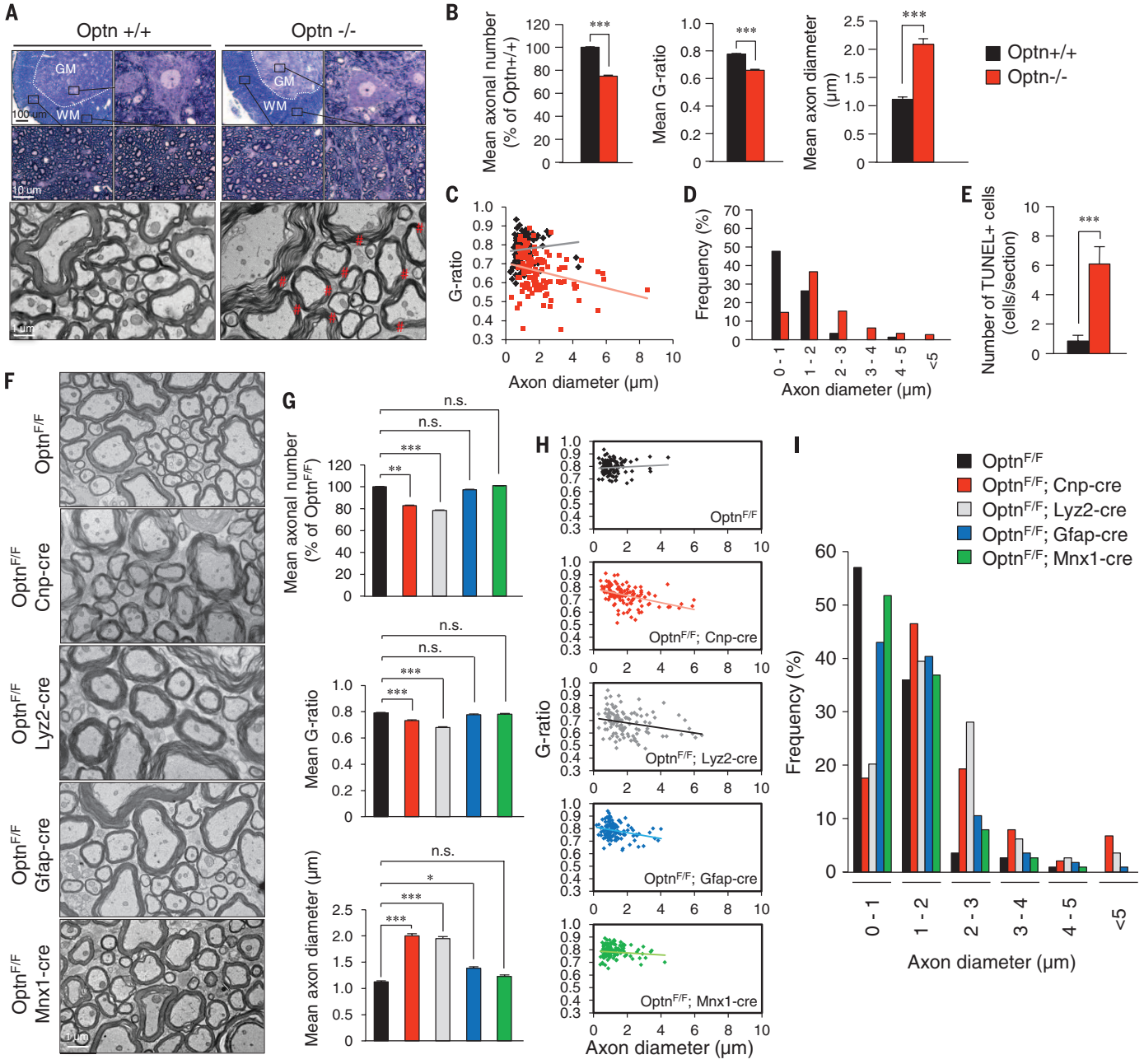

Fig. 1. Optn deficiency in oligodendrocyte and myeloid lineages promotes axonal loss and dysmyelination in the spinal cords of *Optn*$^{-/-}$ mice. (**A**) (Top) Toluidine blue–stained sections from the ventrolateral lumbar spinal cords of WT and *Optn*$^{-/-}$ mice. The boxes show axons in the ventrolateral lumbar spinal cord white matter and the motor neurons in the ventral lumbar spinal cord gray matter, respectively. (Bottom) Electron microscopic analysis of motor axonal myelination in the ventrolateral lumbar spinal cords from WT and *Optn*$^{-/-}$ mice. (**B** to **D** and **F** to **I**) The mean axonal numbers, mean g-ratios, and mean axonal diameters; individual g-ratio distribution; and distributions of axonal diameters in the ventrolateral lumbar spinal cord white matter (L1 to L4) of WT, *Optn*$^{-/-}$ mice, *Optn*$^{F/F}$ mice, *Optn*$^{F/F}$;*Cnp-cre* mice, *Optn*$^{F/F}$;*Lyz2-cre* mice, *Optn*$^{F/F}$;*Gfap-cre* mice, and *Optn*$^{F/F}$;*Mnx1-cre* mice, as indicated. (**E**) The number of TUNEL^{+} cells in the lumbar spinal cords (L1 to L4, one section each) of indicated genotype (five mice for each genotype).

(Fig. 2F). Thus, OPTN might control sensitivity to necroptosis by regulating proteasomal turnover of RIPK1.

Phospho-Ser$^{14/15}$, a marker of Ripk1 activation, was increased in *Optn*$^{-/-}$ microglia relative to WT microglia, which were inhibited by Nec-1s and *Ripk1*$^{D138N/D138N}$ mutation (Fig. 2G). Because microglia express little MLKL, we hypothesize that Ripk1 activation in microglia promotes inflammatory signaling not necroptosis. Consistent with this notion, we detected an increased production of multiple proinflammatory cytokines—including interleukins IL-1α, IL-1β, IL-2, and IL-12; interferon-γ (IFN-γ); and TNFα in the spinal cords of *Optn*$^{-/-}$ mice—which were markedly reduced in the *Optn*$^{-/-}$;*Ripk1*$^{D138N/D138N}$ mice (Fig. 2H). In addition, *Optn*$^{-/-}$ microglia had elevated TNFα, which was inhibited by Nec-1s (fig. S5A). As predicted, the levels of TNFα were also increased in the spinal cords of *Optn*$^{F/F}$;*Lyz2-cre* mice (fig. S5B).

To explore the effect of Optn deficiency on transcriptions, we performed RNA sequencing on WT, *Optn*$^{-/-}$, and *Optn*$^{-/-}$;*Ripk1*$^{D138N/D138N}$ primary microglia. Coexpression analysis (*25*) identified a module with ~1300 genes (ME1) differentially expressed between WT and *Optn*$^{-/-}$ microglia and suppressed by *Ripk1*$^{D138N/D138N}$.

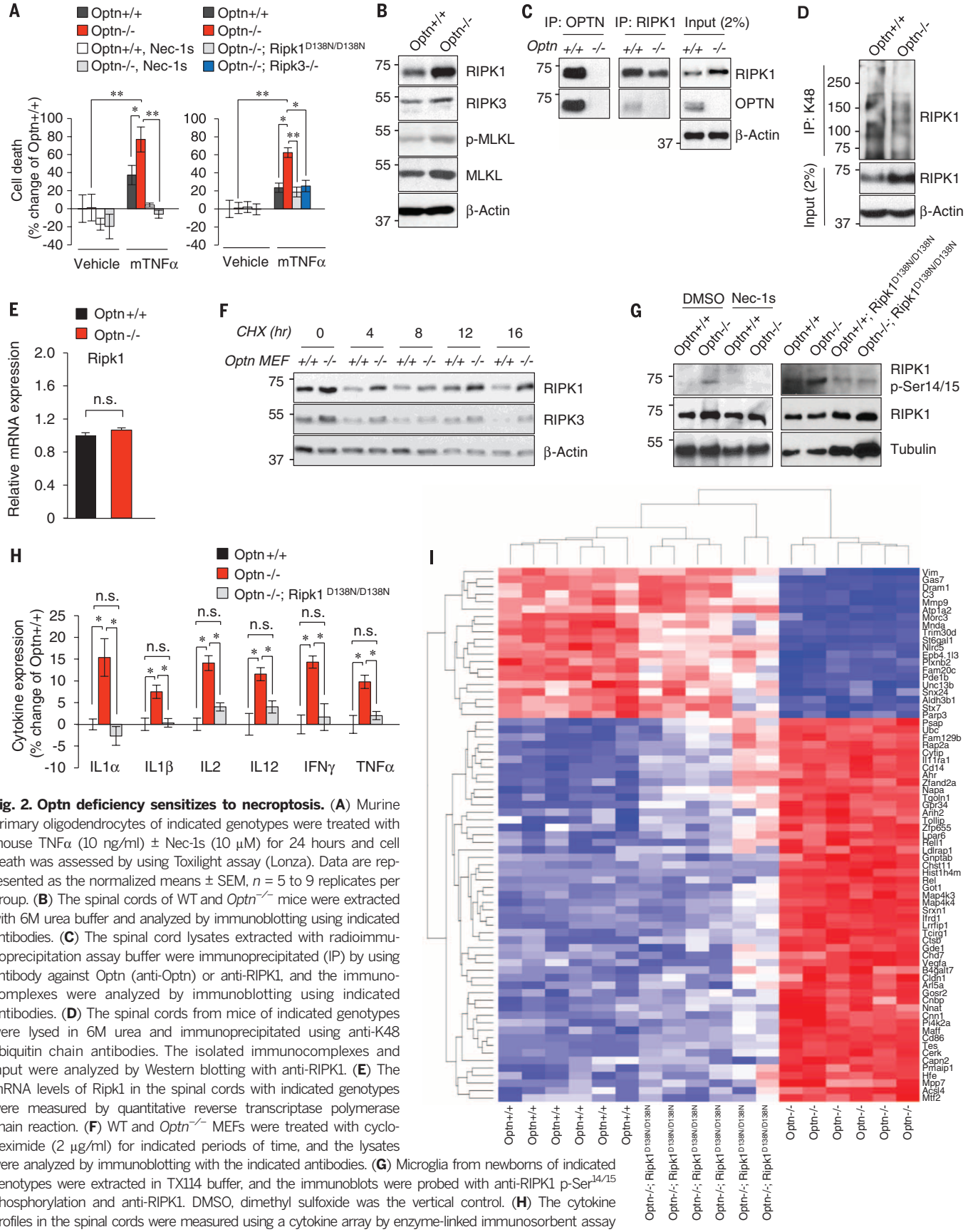

Fig. 2. Optn deficiency sensitizes to necroptosis. (**A**) Murine primary oligodendrocytes of indicated genotypes were treated with mouse TNFα (10 ng/ml) ± Nec-1s (10 μM) for 24 hours and cell death was assessed by using Toxilight assay (Lonza). Data are represented as the normalized means ± SEM, $n = 5$ to 9 replicates per group. (**B**) The spinal cords of WT and *Optn*$^{-/-}$ mice were extracted with 6M urea buffer and analyzed by immunoblotting using indicated antibodies. (**C**) The spinal cord lysates extracted with radioimmunoprecipitation assay buffer were immunoprecipitated (IP) by using antibody against Optn (anti-Optn) or anti-RIPK1, and the immunocomplexes were analyzed by immunoblotting using indicated antibodies. (**D**) The spinal cords from mice of indicated genotypes were lysed in 6M urea and immunoprecipitated using anti-K48 ubiquitin chain antibodies. The isolated immunocomplexes and input were analyzed by Western blotting with anti-RIPK1. (**E**) The mRNA levels of Ripk1 in the spinal cords with indicated genotypes were measured by quantitative reverse transcriptase polymerase chain reaction. (**F**) WT and *Optn*$^{-/-}$ MEFs were treated with cycloheximide (2 μg/ml) for indicated periods of time, and the lysates were analyzed by immunoblotting with the indicated antibodies. (**G**) Microglia from newborns of indicated genotypes were extracted in TX114 buffer, and the immunoblots were probed with anti-RIPK1 p-Ser$^{14/15}$ phosphorylation and anti-RIPK1. DMSO, dimethyl sulfoxide was the vertical control. (**H**) The cytokine profiles in the spinal cords were measured using a cytokine array by enzyme-linked immunosorbent assay (ELISA). (**I**) Heat map of the top 71 genes in the module ME1 differentially expressed in microglia of indicated genotypes. Low expression is shown in blue and high expression, in red.

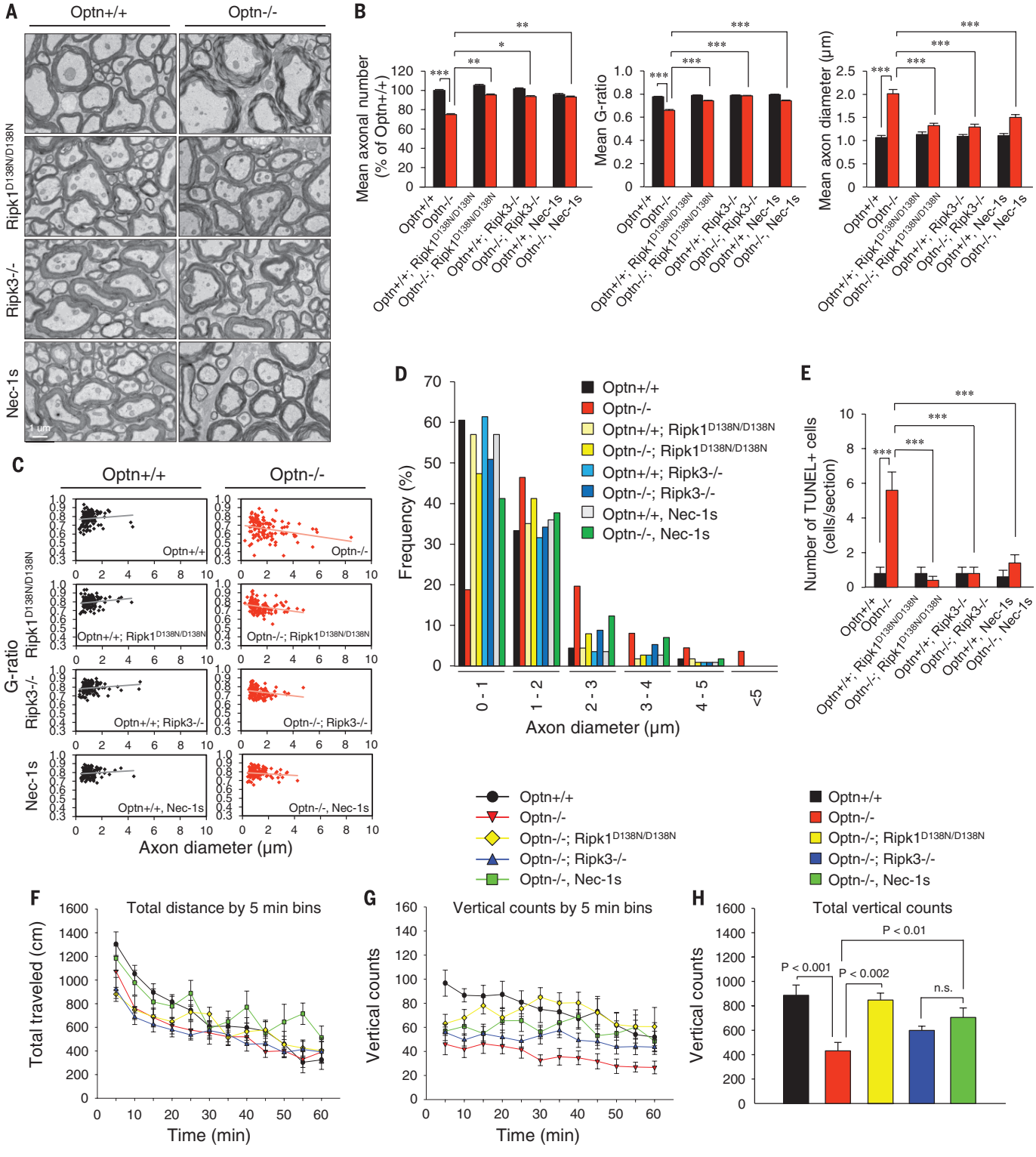

Fig. 3. Ripk1 and Ripk3 mediate axonal pathology in the spinal cords of *Optn*$^{-/-}$ mice. (**A**) Dysmyelination in the spinal cords of *Optn*$^{-/-}$ mice was blocked by genetically inhibiting Ripk1 in *Optn*$^{-/-}$;*Ripk1*$^{D138N/D138N}$ mice, pharmacologically inhibiting Ripk1 by Nec-1s (oral dosing of Nec-1s for 1 month starting from 8 weeks of age), and by loss of Ripk3 in *Optn*$^{-/-}$;*Ripk3*$^{-/-}$ mice. (**B** to **D**) Mean axonal numbers, g-ratios, and axonal diameters (B); individual g-ratio distributions (C); and axonal diameter distributions (D). (**E**) The number of TUNEL^{+} cells in the lumbar spinal cords (L1 to L4, one section each) of indicated genotypes at 3 months of age (five mice per genotype). (**F** to **H**) Mice of indicated genotypes were tested in open-field test for spontaneous motor activity. The mice were at 3 months of age and 28 to 32 g of body weight (no statistically significant difference in body weight between different groups). The total distance traveled in 1 hour showed no difference between different groups (F). *Optn*$^{-/-}$ mice showed a significant deficit on the vertical rearing activity (frequency with which the mice stood on their hind legs). This deficit was blocked after dosing with Nec-1s for 1 month starting from 8 weeks old and in *Optn*$^{-/-}$;*Ripk1*$^{D138N/D138N}$ double-mutant mice and reduced in *Optn*$^{-/-}$;*Ripk3*$^{-/-}$ double-mutant mice (G and H).

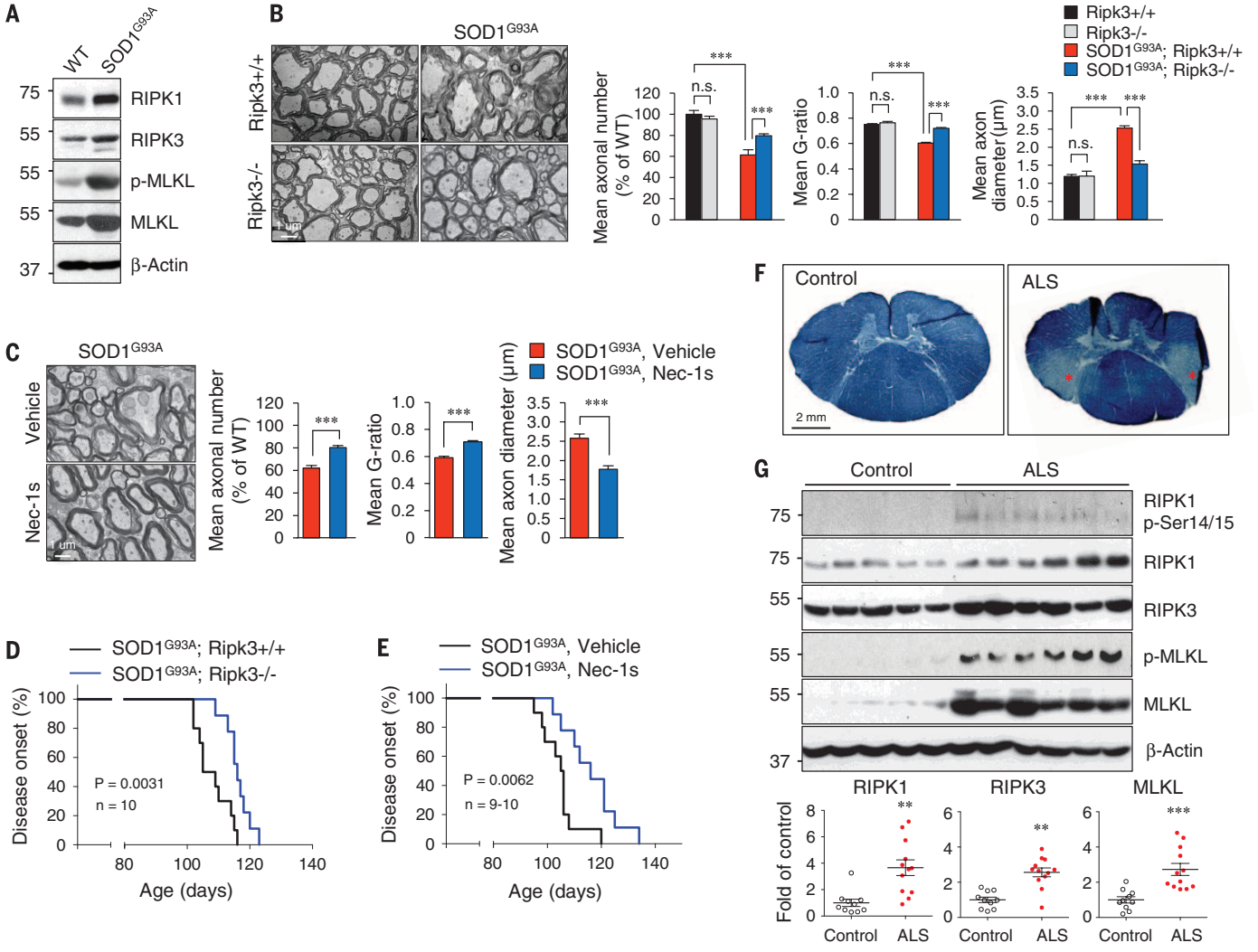

Fig. 4. RIPK1- and RIPK3-mediated axonal pathology is a common mechanism in ALS. (**A**) Urea buffer lysates of spinal cords from WT and *SOD1*^{G93A} transgenic mice (12 weeks of age) were analyzed by immunoblotting using indicated antibodies. (**B** and **C**) The myelination morphology (top), mean axonal numbers (bottom), mean g-ratios (bottom), mean axonal diameters (bottom) of the ventrolateral lumbar spinal cord white matter of *SOD1*^{G93A} mice, *SOD1*^{G93A};*Ripk3*$^{-/-}$ mice (12 weeks of age), and *SOD1*^{G93A} mice dosed with vehicle or Nec-1s for 1 month starting from 8 weeks of age. (**D** and **E**) Ripk3 deficiency (D) and inhibition of Ripk1 by Nec-1s starting from 8 weeks of age (E) delayed the onset of motor dysfunction in *SOD1*^{G93A} mice. (**F**) Sections of pathological spinal cords from a human control and an ALS patient were stained with Luxol fast blue for myelin to show reduced myelination in the lateral column of lower spinal cords of ALS patients. (**G**) Immunoblotting analysis of human control and ALS spinal cord samples using indicated antibodies (top) and the quantification of RIPK1, RIPK3, and MLKL levels from 10 controls and 13 ALS patients (bottom).

The top 71 genes in this module include CD14 and CD86, biomarkers for the proinflammatory M1-like state (*26*) (Fig. 2I and table S2). Elevated CD14 and CD86 in *Optn*$^{-/-}$ microglia were suppressed by Nec-1s and *Ripk1*$^{D138N/D138N}$ (fig. S5C). Thus, Optn deficiency promotes an M1-like inflammatory microglia.

We analyzed the genes differentially expressed in *Optn*$^{-/-}$ microglia using MSigDB (Molecular Signatures Database) (*27*) to identify transcription factors with targets that were overrepresented. We found a significant overrepresentation of the predicted Sp1 transcription factor targets in the ME1 module (table S3) with a network (*28*) of 225 Sp1 targets regulated by RIPK1 (fig. S6A). Increased production of TNFα and the death of L929 cells were blocked by knockdown of Sp1 and by Nec-1s (fig. S6, B and C). Thus, loss of Optn in the spinal cord may increase RIPK1-dependent inflammation.

We examined the involvement of necroptosis in *Optn*$^{-/-}$ mice in vivo. The increase in TUNEL^{+} cells and the axonal pathology of *Optn*$^{-/-}$ mice were all rescued in the *Optn*$^{-/-}$;*Ripk1*$^{D138N/D138N}$ double-mutant and the *Optn*$^{-/-}$;*Ripk3*$^{-/-}$ double-mutant mice and by Nec-1s (Fig. 3, A to E). Behaviorally, *Optn*$^{-/-}$ mice showed no difference in total locomotor activity, whereas the vertical rearing activity was significantly reduced compared with that of WT mice (Fig. 3, F to H). Thus, Optn deficiency leads to hindlimb weakness. Furthermore, the vertical rearing deficit in *Optn*$^{-/-}$ mice was rescued pharmacologically by Nec-1s and genetically in the *Optn*$^{-/-}$;*Ripk1*$^{D138N/D138N}$ mice and *Optn*$^{-/-}$;*Ripk3*$^{-/-}$ mice. Thus, Optn deficiency leads to the activation of necroptotic machinery to promote axonal pathology.

To explore the involvement of RIPK1-mediated axonal pathology in ALS in general, we used *SOD1*^{G93A} transgenic mice. Oligodendrocytes in *SOD1*^{G93A} mice degenerate early, but the mechanism is unclear (*29*). We found that the expression of Ripk1, Ripk3, and MLKL in the spinal cords of *SOD1*^{G93A} transgenic mice was elevated (Fig. 4A). In addition, we observed a similar axonal pathology as that of *Optn*$^{-/-}$ mice in *SOD1*^{G93A} mice before the onset of motor dysfunction (Fig. 4, B and C). Furthermore, these axonal myelination defects were blocked and motor dysfunction onset was delayed genetically by *Ripk3* knockout or by oral administration

of Nec-1s (Fig. 4, D and E). Thus, although we cannot rule out the contribution of Ripk1 or other proapoptotic factors to the degeneration of motor neuron cell bodies (*30*, *31*), the activation of necroptosis contributes to axonal pathology and motor dysfunction in the $SOD1^{G93A}$ transgenic mice.

We next characterized the role of RIPK1 and necroptosis in human ALS. We found evidence of demyelination in the lateral column white matter of lower spinal cord pathological samples from ALS patients as reported (Fig. 4F). In human ALS pathological samples, we also detected multiple biochemical hallmarks of necroptosis, including increased levels of RIPK1, RIPK3, and MLKL and increased RIPK1 p-$Ser^{14/15}$ and p-MLKL in both microglia and oligodendrocytes (Fig. 4G, fig. S7, and table S4). Note that p-MLKL was primarily localized in the white matter, where demyelination was found.

Taken together, our results provide a direct connection between Wallerian-like degeneration induced by OPTN deficiency and RIPK1-regulated necroptosis and inflammation. By promoting both inflammation and cell death, RIPK1 may be a common mediator of axonal pathology in ALS (fig. S8). Because RIPK1 is recruited specifically to the TNF receptor TNFR1 to mediate the deleterious effect of TNFα (*32*), blocking RIPK1 may provide a therapeutic option for the treatment of ALS without affecting TNFR2. Finally, given the recruitment of OPTN to intracellular protein aggregates found in pathological samples from patients with Alzheimer's disease, Parkinson's disease, Creutzfeldt-Jakob disease, multiple system atrophy, and Pick's disease (*33*, *34*), a possible role of RIPK1 in mediating the wide presence of axonal degeneration in different neurodegenerative diseases should be considered.

REFERENCES AND NOTES

1. E. Beeldman *et al.*, *Amyotroph. Lateral Scler. Frontotemporal Degener.* **16**, 410–411 (2015).
2. E. T. Cirulli *et al.*, *Science* **347**, 1436–1441 (2015).
3. H. Maruyama *et al.*, *Nature* **465**, 223–226 (2010).
4. I. Munitic *et al.*, *J. Immunol.* **191**, 6231–6240 (2013).
5. G. Zhu, C. J. Wu, Y. Zhao, J. D. Ashwell, *Curr. Biol.* **17**, 1438–1443 (2007).
6. D. Ofengeim, J. Yuan, *Nat. Rev. Mol. Cell Biol.* **14**, 727–736 (2013).
7. S. He *et al.*, *Cell* **137**, 1100–1111 (2009).
8. L. Sun *et al.*, *Cell* **148**, 213–227 (2012).
9. D. W. Zhang *et al.*, *Science* **325**, 332–336 (2009).
10. A. Degterev *et al.*, *Nat. Chem. Biol.* **4**, 313–321 (2008).
11. A. Degterev *et al.*, *Nat. Chem. Biol.* **1**, 112–119 (2005).
12. L. Conforti, J. Gilley, M. P. Coleman, *Nat. Rev. Neurosci.* **15**, 394–409 (2014).
13. M. C. Raff, A. V. Whitmore, J. T. Finn, *Science* **296**, 868–871 (2002).
14. J. T. Wang, Z. A. Medress, B. A. Barres, *J. Cell Biol.* **196**, 7–18 (2012).
15. S. Sasaki, S. Maruyama, *J. Neurol. Sci.* **110**, 114–120 (1992).
16. L. Zhuo *et al.*, *Genesis* **31**, 85–94 (2001).
17. B. E. Clausen, C. Burkhardt, W. Reith, R. Renkawitz, I. Förster, *Transgenic Res.* **8**, 265–277 (1999).
18. C. Lappe-Siefke *et al.*, *Nat. Genet.* **33**, 366–374 (2003).
19. C. N. Parkhurst *et al.*, *Cell* **155**, 1596–1609 (2013).
20. D. E. Christofferson, J. Yuan, *Curr. Opin. Cell Biol.* **22**, 263–268 (2010).
21. J. Hitomi *et al.*, *Cell* **135**, 1311–1323 (2008).
22. D. E. Christofferson *et al.*, *Cell Death Dis.* **3**, e320 (2012).
23. A. Polykratis *et al.*, *J. Immunol.* **193**, 1539–1543 (2014).
24. D. Ofengeim *et al.*, *Cell Rep.* **10**, 1836–1849 (2015).
25. P. Langfelder, S. Horvath, *BMC Bioinformatics* **9**, 559 (2008).
26. K. A. Kigerl *et al.*, *J. Neurosci.* **29**, 13435–13444 (2009).
27. A. Subramanian *et al.*, *Proc. Natl. Acad. Sci. U.S.A.* **102**, 15545–15550 (2005).
28. S. I. Berger, J. M. Posner, A. Ma'ayan, *BMC Bioinformatics* **8**, 372 (2007).
29. S. H. Kang *et al.*, *Nat. Neurosci.* **16**, 571–579 (2013).
30. D. B. Re *et al.*, *Neuron* **81**, 1001–1008 (2014).
31. T. W. Gould *et al.*, *J. Neurosci.* **26**, 8774–8786 (2006).
32. J. J. Peschon *et al.*, *J. Immunol.* **160**, 943–952 (1998).
33. T. Osawa *et al.*, *Neuropathology* **31**, 569–574 (2011).
34. H.-X. Deng *et al.*, *Arch. Neurol.* **68**, 1057–1061 (2011).

ACKNOWLEDGMENTS

We thank B. Caldarone of the NeuroBehavior Laboratory, Harvard Institute of Medicine, for conducting mouse behavior analysis; J. Walters at the Harvard Medical School Nikon microscope facility for fluorescence microscopy; and M. Ericsson of the Electron Microscopy Facility at Harvard Medical School for analysis. This work was supported in part by grants from the National Institute of Neurological Disorders and Stroke (1R01NS082257) and the National Institute on Aging (1R01AG047231), NIH; and by the National Science and Technology Major Project of China (2014ZX09102001-002) and State Key Program of National Natural Science of China (no. 31530041) (to J.Y.); National Institute of Allergy and Infectious Diseases (2RO1AI075118) (to M.A.K.); European Research Council Advanced Grants (grant agreement no. 323040) (to M.P.) and Target ALS (to J.R.). Y.I. was supported in part by postdoctoral fellowships from Japan (Daiichi Sankyo Foundation of Life Science, The Nakatomi Foundation, the Mochida Memorial Foundation for Medical and Pharmaceutical Research, and Japan Society for the Promotion of Science). D.O. was supported by a postdoctoral fellowship from the National Multiple Sclerosis Society and a National Multiple Sclerosis Society Career Transition Award. H.C. was supported by a grant from Huazhong University of Science and Technology, Wuhan, China. $Ripk3^{-/-}$ mice and K48 ubiquitin antibodies are available from V. Dixit under a material transfer agreement with Genentech. $Ripk1^{D138N}$ mice are available from M. Pasparakis of University of Cologne, Germany, under a material transfer agreement with University of Cologne. J.Y. is an inventor on U.S. patent 7,491,743 B2 held by Harvard University that covers 7-Cl-O-Nec-1.

SUPPLEMENTARY MATERIALS

www.sciencemag.org/content/353/6299/603/suppl/DC1
Materials and Methods
Figs. S1 to S8
Tables S1 to S4
References (*35*–*40*)

13 March 2016; accepted 7 July 2016
10.1126/science.aaf6803

Editor's Summary

Axonal pathology and necroptosis in ALS

Necroptosis, a non–caspase-dependent form of cell death, can be reduced in disease states by inhibiting a kinase called RIPK1. Until now, no human mutations have been linked to necroptosis. Ito *et al.* show that loss of optineurin, which is encoded by a gene that has been implicated in the human neurodegenerative disorder ALS (amyotrophic lateral sclerosis), results in sensitivity to necroptosis and axonal degeneration. When RIPK1-kinase dependent signaling is disrupted in mice that lack optineurin, necroptosis is inhibited and axonal pathology is reversed.

Science, this issue p. 603